2022 IEEE 95th Vehicular Technology Conference (VTC2022-Spring) | 978-1-6654-8243-1/22/$31.00 ©2022 IEEE | DOI: 10.1109/VTC2022-Spring54318.2022.9860514

Compressive-Sampling Spectrum Scanning with a Beamforming Receiver for Rapid, Directional, Wideband Signal Detection

Petar Barac, *Student, IEEE,* Matthew Bajor, *Member, IEEE,* and Peter R. Kinget *Fellow, IEEE,*
Columbia University, New York, NY, 10027, USA

***Abstract*—Communication systems across a variety of applications are increasingly using the angular domain to improve spectrum management. They require new sensing architectures to perform energy-efficient measurements of the electromagnetic environment that can be deployed in a variety of use cases. This paper presents the Directional Spectrum Sensor (DSS), a compressive sampling (CS) based analog-to-information converter (CS-AIC) that performs spectrum scanning in a focused beam. The DSS offers increased spectrum sensing sensitivity and interferer tolerance compared to omnidirectional sensors. The DSS implementation uses a multi-antenna beamforming architecture with local oscillators that are modulated with pseudo random waveforms to obtain CS measurements. The overall operation, limitations, and the influence of wideband angular effects on the spectrum scanning performance are discussed. Measurements on an experimental prototype are presented and highlight improvements over single antenna, omnidirectional sensing systems.**

***Index Terms*—Spectrum sensing, Compressive Sampling, Angular Spectrum Sensing, Beamforming,Phased Array, Cognitive Radio**

I. Introduction

THE growth of wireless connectivity has forced electronic devices to operate in increasingly congested EM environments. Whether interference comes from environmental noise, adversarial jamming or co-channel effects, wireless systems must be able to detect and adapt to the environment without any a priori knowledge of the interferers. These EM aware receivers utilize the time, frequency, and direction of signals to survey the EM environment. For example, systems such as UAVs will require line-of-sight (LOS) links and therefore require the ability to sense and select channels based both on the spectrum availability and angular availability [1]. The angular domain has also been growing in importance with the rising operating frequencies, e.g. in mmWave devices, where the propagation losses are too high to operate without using beamforming [2] [3].

Rapid spectrum scanners using compressive sampling (CS) have been developed to detect which spectral bins are occupied by a signal or interferer. These systems include the MWC [4], the QAIC [5], and the DRF2IC [6] which were only implemented for use with a single antenna and operate omnidirectionally; they do not provide any angular information on signals. Rapid angular sensing at a given operating frequency has been realized using CS in the DSIC [7] , but it is unable

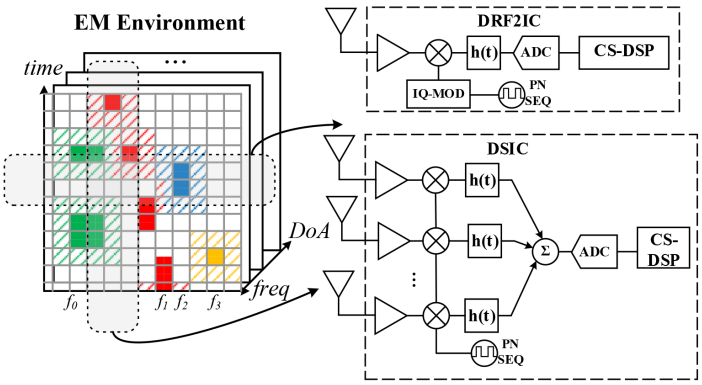

Fig. 1: An illustration of a cluttered RF environment in the angular, frequency and time domains. Also shown are the applicable sensor architectures for sensing signals in a particular domain.

to do spectrum sensing. Fig. 1 graphically illustrates the task of multi-domain EM sensing; the three domains of interest are represented as discrete bins of time, frequency and angle or direction of arrival (DoA). Also shown are the applicable CS sensor architectures to each sensing domain.

Unlike traditional scanners that exhaustively search every frequency or DoA bin, CS-based sensors are able to rapidly scan and locate the occupied frequency or DoA bin with fewer scans. This property also results in these architectures consuming less power per scan than traditional scanners.

This paper demonstrates a realized hardware system called the *Directional Spectrum Sensor* (DSS) that allows for energy-efficient wideband spectrum sensing to occur at specific directions using CS and beamforming techniques, merging both the frequency and angular sensing domains for highly efficient and interferer tolerant sensing.

II. Problem Formulation

While there are many challenges with operating a receiver in a cluttered RF environment, most problems fall into two categories. The first is the need to rapidly scan the RF environment in either the spectral or angular domains to determine the locations and strength of interferers. In order to tackle this problem in the spectral domain, architectures such as the QAIC [5] and DRF2IC [6] have been designed that can rapidly detect interferers using CS. While both are capable

of detecting several interferers over a instantaneous bandwidth of 1 GHz in microseconds, they are limited by their single antenna, omnidirectional architecture making them unsuitable for scenarios where angular information is needed.

The second challenge is that once an interferer is found, it must be handled in such a way that its presence does not adversely effect the operational characteristics of the radio receiver. Large interferers can act as blockers and desensitize the receiver's ability to detect other weaker signals in the same band. An effective way to improve receiver sensitivity and to remove the effects of the large interferer is to use multiple antennas and to destructively sum the interferer before its effects propagate through the receiver chain. Fig. 2 shows how the larger interferer $S_2(t)$ is spatially filtered out, allowing the receiver to detect the weak signal $S_1(t)$. The multiple antenna system is able to control the number of signals that are present at the receiver.

A solution to these challenges will require combining the ability to rapidly scan the RF environment for interferers with the ability to control which direction of the RF environment is being scanned.

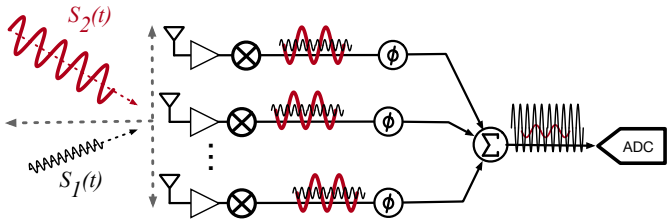

Fig. 2: Angular filtering of large interferers to improve sensitivity in the a specific direction of interest

III. Theory of Operation of the Directional Spectrum Scanner

A new architecture called the Directional Spectrum Scanner or DSS solves both challenges in one unified system. The DSS is able to scan a wide spectrum while simultaneously utilizing angular information of interfering signals to null them before adverse effects on the receiver can take place. The scanner utilizes CS spectrum sensing and N_a antenna elements in an overall compact hardware architecture that is similar to a conventional beamformer (CBF). Table I outlines the system parameters that will be used for the rest of this paper.

TABLE I: DSS System Parameters

Parameter	Description
f_c	Center of the Frequency Band of Interest
f_{min}, f_{max}	Minimum and Maximum Frequency of Band of Interest
B	Bandwidth of Individual Spectral Bin
N	Number of Spectral Bins
m	Number of measurements
K	Number of signals of interest present
θ_{steer}	Direction of Antenna Array Main Beam
N_a	Number of antennas
d	Array Element Spacing

A. Compressive Sampling for Wideband Spectrum Sensing

The DSS uses CS [1] to be able to perform a spectrum scan in a much shorter amount of time than Nyquist based spectrum sensing systems. By exploiting a property of the spectrum called *sparsity*, the DSS can find K interferers in as little as m measurements compared to N measurements with a Nyquist based system where $N > m$. Sparsity is defined as $N \gg K$ where N is the number of possible signal locations (spectral bins) with bandwidth B and K is the number of bins with an interferer above a threshold τ [8]. The number of random CS measurements m is defined as

$$m = C_0 K \log_{10} \frac{N}{K}, \; 2 \leq C_0 \leq 4 \tag{1}$$

For the DSS, m random measurements make up the sensing matrix $\mathbf{\Phi}$.

The $\mathbf{x}$ vector consists of time samples and can be represented as the sparse $\mathbf{X}$ vector being multiplied by $\mathbf{\Psi}$, a *DFT*-like dictionary matrix of size $N \times N$.

$$y = \Phi \Psi X \tag{2}$$

The y matrix is the result of the linear projections of $\mathbf{\Phi}$ on $\mathbf{x}$, where the y matrix is $m \times n_s$ sized (n_s representing the number of time samples collected) and the represents the measurements that are collected at the output of the DSS.

Using the collected measurements and the sensing and dictionary matrix, the nonzero entries of $\mathbf{X}$ can be recovered using convex optimization methods such as Orthogonal Matching Pursuit (OMP) [9]. It should be noted that recovering the spectral locations of interferers above τ does not require fully reconstructing the incident signal.

B. DSS Architecture

While most spectrum sensing architectures require the use of multiple baseband branches implemented in physical hardware, [6], [5], the DSS is able to utilize N_a antennas and a single CS measurement hardware branch.

Fig. 3 shows the overall system architecture of the directional spectrum scanner. The DSS is built upon a beamforming receiver where each antenna path is able to shift the relative phase with respect to other paths; the key difference is the modulated LO supplied to each mixer which allows for CS spectral measurements to be collected.

The DSS uses a uniform linear array (ULA) with an antenna spacing d of $\frac{\lambda_c}{2}$. Each antenna is an omnidirectional dipole that is connected to a low noise amplifier (LNA). In each antenna path n, the complex mixer is able to mix the received RF signal $x_n(t)$ with either a sinusoidal LO for regular signal reception or with a pseudo-random bit sequence (PRBS) modulated LO for wideband sensing. When using a PRBS modulated LO, energy is collected from across a wide spectral band to form a compressive sample [6] as shown in Fig. 4 where a single antenna path of the DSS is shown.

[1]Compressive sampling is briefly introduced in this paper, for a more in-depth introduction and other CS hardware architectures refer to [4]–[8].

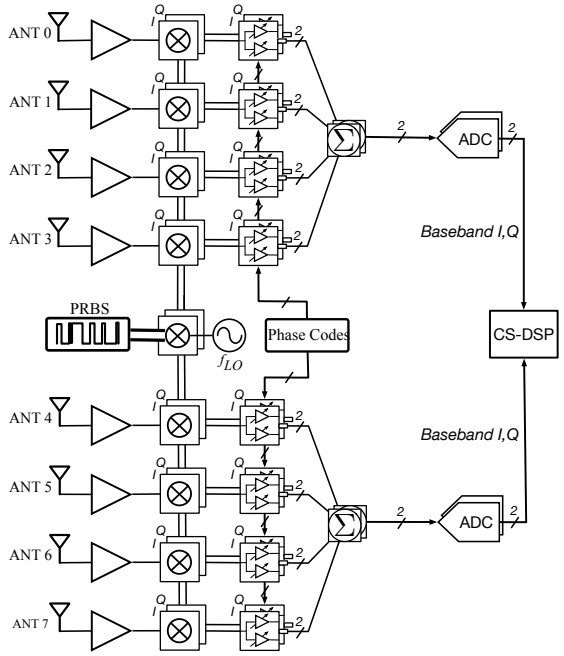

Fig. 3: The overall architecture of the Directional Spectrum Scanner (DSS). The prototype chip has 8 antenna paths that sum into two outputs.

The PRBS waveform generator creates the baseband waveform that mixes with the LO. The PRBS waveform generator operates at clock frequency f_{PRBS} and with a length of $N = 127$ bits and the LO operates at f_c. The PRBS modulated LO is distributed to the mixer in each antenna path with phase-matched transmission lines.

The spectrum of the PRBS modulated LO is a series of tones centered at f_c spaced $\frac{f_{PRBS}}{N}$ apart from each other with a 3 dB response from $f_{min} = f_c - \frac{f_{PRBS}}{2}$ to a $f_{max} = f_c + \frac{f_{PRBS}}{2}$. This response mixes down the RF signal $X(f)$ to baseband. The f_{PRBS} determines the frequency range of the spectrum scan and the length of the sequence determines the number of bins N being scanned over. The resolution of each spectral bin is $B = \frac{f_{PRBS}}{N}$.

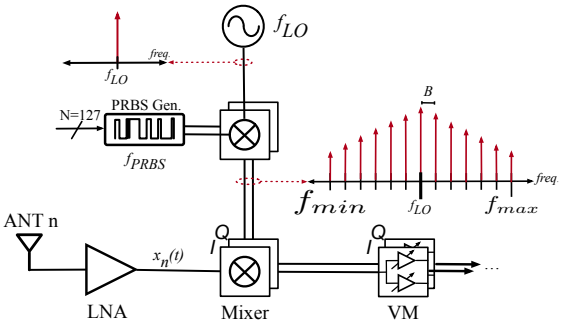

Fig. 4: Illustration of a single antenna path of the DSS. The spectrum of the PRBS modulated LO is a series of tones spaced B apart.

The output of each complex mixer is connected to a vector modulator (VM) that controls the amplitude and phase shift of each antenna path at baseband. The VMs are used to constructively and destructively sum all 8 antenna paths to steer the main beam of the array in the angular domain.

Due to the array spacing d and the angle of arrival θ of RF signal normal to the array, the received RF signal in each path $x_n(t)$ will have a progressive time delay between each element as a result. The time delay at antenna path n is

$$\Delta t_n = \frac{nd \sin\theta}{c} \tag{3}$$

For narrowband signals centered around f_c and an array element spacing of $d = \frac{\lambda_c}{2}$, the time delay at each antenna n can be approximated with a phase shift $e^{-jn\pi \sin\theta}$.

For all 8 paths to sum constructively together into a single baseband output for an angle of arrival θ, the VMs phase shift each antenna path by $e^{jn\pi \sin\theta}$. The ability to apply phase shifts with the VMs allows for this architecture to steer the main beam of the antenna array in the direction of interest and spatially filter out other angles.

C. Branch Expansion

The DSS has 8 antenna paths for angular filtering but only has a single hardware branch for CS measurements. Each mixer in the DSS is using the same PRBS modulated LO and can be treated as one CS hardware branch generating $m = 1$ measurements. Adding more hardware branches would require doubling the size of the entire system as each measurement would need its own dedicated mixer, VM and base band path. This is an inefficient method of obtaining the minimum number of measurements as required by (1) that ties the sensors performance to the overall size of the hardware.

Instead, the required measurements are extracted from a single hardware branch in a method referred to as branch expansion. Similarly, branch expansion enables the DRFIC [6] architecture to detect multiple interferers with only 2 hardware branches. The cost of using branch expansion is that it requires an increased sampling rate of the analog-to-digital (A/D) as well as more complexity in the CS digital signal processing back-end. This is a preferred trade-off over increasing the number of hardware branches in the DSS that enables it to be a compact architecture.

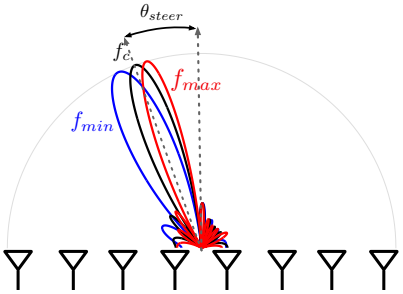

Fig. 5: The beam squint effect on the array factor. The antenna beam corresponding to the edges of the spectrum bandwidth ,f_{min} and f_{max} deviate from the desired direction of θ_{steer}.

D. Bandwidth and Steering Limitations

While each individual antenna path of the DSS can operate over a large bandwidth, the overall bandwidth is limited by the

number array elements N_a , the spacing between the elements d, and the phase shifts implemented via the VMs. These phase shifts approximate the time delay around only a narrowband of frequencies centered around f_c. For frequencies outside this range, the phase shift applied by the VMs creates a frequency dependent array factor response called *beam squint*. This limits the overall bandwidth in phased array systems [10]. A true time delay-line would not impose this limitation on bandwidth but this comes at the expense of the significant hardware complexity.

For a desired θ_{steer}, a phase shift of $e^{jn\pi \sin\theta_{steer}}$ needs to be applied by the VMs to each antenna path n. The error between the desired θ_{steer} and the actual main beam location θ is expressed as

$$\Delta\theta = \arcsin\left(\frac{f_c}{f}\sin\theta_{steer}\right) - \theta_{steer} \tag{4}$$

This error will cause the frequencies at the upper and lower end of the band to have reduced gain from the array factor in the desired direction. Frequencies at the lower end of the band f_{min} will be steered to angles larger than θ_{steer} and frequencies at the higher end of the band f_{max} will be steered to angles lower than θ_{steer}. Figure 5 illustrates this effect. Apart from the reduced gain in the desired direction, beam squint will widen the range of angles across the operating frequencies considered to be in the main beam. This effectively worsens the spatial resolution, which is inconsequential since as long as the beams corresponding to the end of the bands are within the target steering direction, the array is able to spatially filter out signals from other directions.

Using the analysis and relationships from [10], the fractional bandwidth of this system is defined where the beams associated with the frequency bounds of the bandwidth ,f_{max} and f_{min}, are at half power in the intended steering direction. This fractional bandwidth for a ULA with d element spacing is a function of the number of antenna elements and the maximum steering angle, and is given by

$$\frac{\Delta f}{f} = \frac{0.886\lambda_c}{N_a d \sin\theta_{steer}} \tag{5}$$

Increasing the field of view or the number of elements will decrease the range of frequencies that can scanned within a certain beam. For 8 antenna paths spaced with $\frac{\lambda_c}{2}$ and with a constrained the field of view to $\pm 30°$ normal to the array, the DSS can achieve a fractional bandwidth of 0.433. With a f_c of 1.246 GHz, this allows for spectrum sensing to operate in a bandwidth of 540 MHz. This shows that the use of only VMs does not significantly shrink the spectrum sensing bandwidth while keeping hardware complexity low. Using true time delay can overcome these limitations but at added hardware complexity.

IV. Experimental Results

The performance of DSS was evaluated using a realized DSS hardware system and hardware test bed. This test bed simulates an EM environment with signals existing at different frequencies and varying angles of arrival to the test system. The advantages of the DSS operation in this environment will be reinforced by comparing it to a single antenna spectrum sensor. Both the DSS and the single antenna spectrum sensor were tested in the same simulated EM environment. The single antenna system used in this test is the DSS with only one antenna port connected to the test bed. This will allow for a fair comparison of the two systems because they use the same CS spectrum sensing hardware, but only the DSS can spatially filter by using all its antennas paths.

A. Experimental Setup and Test Scenario

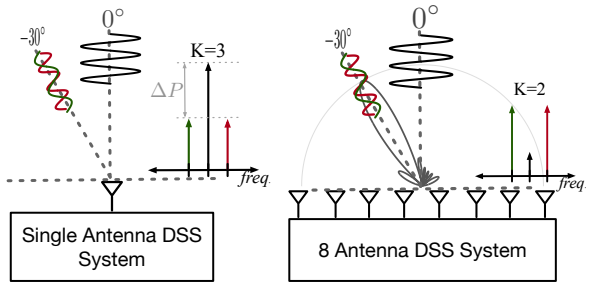

Fig. 6: The single antenna DSS system (left) and the 8 antenna DSS system (right) in the simulated EM test environment.

The hardware test bed emulates up to three different continuous wave tones at up to two angles of arrival simultaneously. The input signals are divided into 8 cables with an incremental phase between the cables, corresponding to the angle of arrival that would be incident to a ULA with $\frac{\lambda_c}{2}$ spacing between elements.

Both systems were evaluated in their ability to detect multiple signals originating from the same direction of arrival with varying signal power levels. In addition, these systems were evaluated on the ability to detect target signals in the presence of a large interferer. Fig. 6 illustrates the simulated test environment that will be used to evaluate the drawbacks of a single antenna system and to demonstrate CS spectrum sensing with spatial filtering. A single tone located at a different frequency will act as an interferer that is incident normal to the array. The two target signals are located at different frequencies than that of the interferer, and are incident at $-30°$ normal to the array. The two target signals were both held at -48 dBm, while the power of the interferer is swept from -8 dBm to -68 dBm, resulting in a power difference (ΔP) ranging from 40 dB to -20 dB between the interferer and target signals. All signal powers are measured at each individual antenna input on the hardware setup.

B. DSS Operating Parameters

The DSS operates at a center frequency, f_c, of 1.246 GHz with a 127 bit long PRBS ($N = 127$) running at a clock speed of $f_{PRBS} = 508$ MHz. This sets the bandwidth of the spectrum sensing to between an f_{min} of 0.992 GHz, and an f_{max} of 1.5 GHz, with frequency bin resolution of $B = 4$ MHz. The output of the DSS is sampled using an ADC with a sampling rate of f_s of 100 MHz.

C. Measurement Results

Fig. 7 shows the probability of detection (P_D) of three signals vs signal power. The three signals are all of equal power and have the same angle of arrival of $-30°$ relative to the normal. The P_D is compared for both the single antenna system and the DSS with its main beam pointed at $-30°$. The single antenna implementation achieves a $P_D > 90\%$ at powers above -55 dBm while the DSS achieves the same P_D at powers above -64 dBm. This increased 9 dB of sensitivity is a result of the DSS using eight antennas over a single antenna.

Fig. 8 illustrates how the single antenna system and the DSS are affected by a high power interferer. Both systems are expected to only detect the two target signals and ignore the presence of the interferer signal. The presence of interferers decreases the single antenna receiver's sensitivity and as a result the target signals are not detected by the sensor. The P_D of the target signals is below 90% when the interferer is 5 dB higher than the two target signals. Once the interferer power approaches that of the target signal, the P_D of the target signal increases above 90%. Even in the case where the interferers fall below the target signal power, the receiver is still tasked with operating in an EM environment with $K = 3$ signals. Clearly, the omnidirectional system's ability to detect the target signal is severely limited by the presence of high power interferers.

In the same EM environment, the DSS is able to minimize the effect of the large interferer. By steering the main beam of the array towards the target signals at $-30°$ and placing a null in the direction of the interferer at $0°$, the P_D for the target signals is now above above 90% for interferer powers up to 30 dB larger than the target signals. The DSS detects only the signals in the main beam of the array and spatially filters the interferer, exhibiting better interferer rejection than the single-antenna receiver.

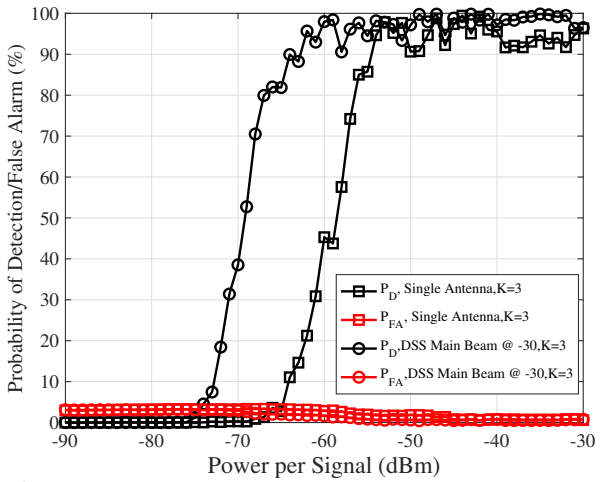

Fig. 7: P_D and P_{FA} as a function of the power per signal for detecting 3 signals using the DSS vs the single antenna system

V. Conclusions

The directional spectrum scanner (DSS) demonstrates the ability to perform rapid wideband CS-based spectrum sensing within a directional beam. Using branch expansion, the overall hardware architecture is compact without trading off performance. Its multi-antenna architecture allows for the DSS to take CS measurements in a focused angular direction and spatially filter interferers while improving detection sensitivity. This allows the DSS to control the sparsity in the frequency domain for more efficient and interferer tolerant directional spectrum sensing.

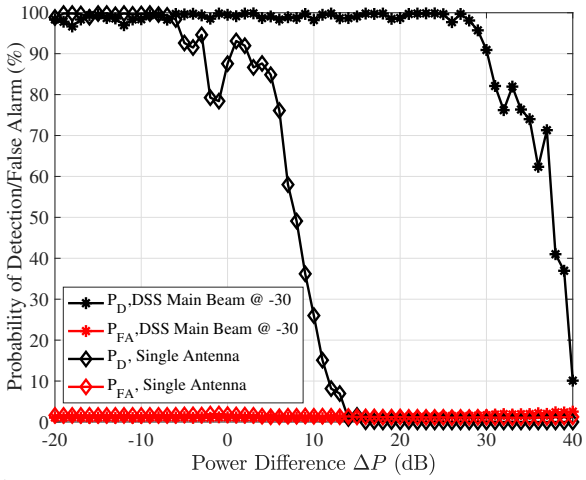

Fig. 8: P_D and P_{FA} as a function of the difference between the power of the target signals and that of the interferer in the single antenna system vs the DSS system.

References

[1] B. Shang, V. Marojevic, Y. Yi, A. S. Abdalla, and L. Liu, "Spectrum sharing for uav communications: Spatial spectrum sensing and open issues," *IEEE Vehicular Technology Magazine*, vol. 15, no. 2, pp. 104–112, June 2020.

[2] W. Roh, J.-Y. Seol, J. Park, B. Lee, J. Lee, Y. Kim, J. Cho, K. Cheun, and F. Aryanfar, "Millimeter-wave beamforming as an enabling technology for 5g cellular communications: Theoretical feasibility and prototype results," *IEEE communications magazine*, vol. 52, no. 2, pp. 106–113, February 2014.

[3] T. S. Rappaport, Y. Xing, O. Kanhere, S. Ju, A. Madanayake, S. Mandal, A. Alkhateeb, and G. C. Trichopoulos, "Wireless communications and applications above 100 ghz: Opportunities and challenges for 6g and beyond," *IEEE access*, vol. 7, pp. 78 729–78 757, June 2019.

[4] M. Mishali and Y. C. Eldar, "From theory to practice: Sub-nyquist sampling of sparse wideband analog signals," *IEEE Journal of selected topics in signal processing*, vol. 4, no. 2, pp. 375–391, 2010.

[5] R. T. Yazicigil, T. Haque, M. R. Whalen, J. Yuan, J. Wright, and P. R. Kinget, "Wideband rapid interferer detector exploiting compressed sampling with a quadrature analog-to-information converter," *IEEE Journal of Solid-state circuits*, vol. 50, no. 12, pp. 3047–3064, August 2015.

[6] T. Haque, M. Bajor, Y. Zhang, J. Zhu, Z. A. Jacobs, R. B. Kettlewell, J. Wright, and P. R. Kinget, "A reconfigurable architecture using a flexible lo modulator to unify high-sensitivity signal reception and compressed-sampling wideband signal detection," *IEEE Journal of Solid-State Circuits*, vol. 53, no. 6, pp. 1577–1591, June 2018.

[7] M. Bajor, T. Haque, J. Wright, and P. R. Kinget, "Theory and design of a direct space-to-information converter for rapid detection of interferer doa," in *2017 IEEE 86th Vehicular Technology Conference (VTC-Fall)*. IEEE, September 2017, pp. 1–5.

[8] E. J. Candès, "Compressive sampling," in *Proceedings of the International Congress of Mathematicians*, vol. 3, August, pp. 1433–1452.

[9] J. A. Tropp and A. C. Gilbert, "Signal recovery from random measurements via orthogonal matching pursuit," *IEEE Transactions on information theory*, vol. 53, no. 12, pp. 4655–4666, December 2007.

[10] R. Mailloux, *Phased Array Antenna Handbook, Third Edition*, ser. Artech House antennas and electromagnetics analysis library. Artech House Publishers, 2017.